Michigan State University

National Superconducting Cyclotron Laboratory

SIGN DEPENDENCE OF SPIN POLARIZATION FOR SECONDARY FRAGMENTS PRODUCED FOLLOWING INTERMEDIATE-ENERGY PROJECTILE FRAGMENTATION

P.F. MANTICA, R.W. IBBOTSON, D.W. ANTHONY,
M. FAUERBACH, D.J. MORRISSEY, C.F. POWELL,
J. RIKOVSKA, M. STEINER, N.J. STONE, and W.B. WALTERS

MSUCL-1063

MARCH 1997

Sign dependence of spin polarization for secondary fragments produced following intermediate-energy projectile fragmentation

P. F. Mantica[1,2], R. W. Ibbotson[2], D. W. Anthony[2], M. Fauerbach[2], D. J. Morrissey[1,2], C. F. Powell[2], J. Rikovska[3,4], M. Steiner', N. J. Stone[3], and W. B. Walters[4]

[1] *Department Of Chemistry, Michigan State University, East Lansing, Michigan* 48824

[2] *National Superconducting Cyclotron Laboratory, Michigan State University, East Lansing, Michigan 48824*

[3] ***Department*** of ***Physics, Oxford University, Oxford OX1 3PU, United*** Kingdom

[4] ***Department of Chemistry*** and ***Biochemistry,*** University *of* ***Maryland, College Park, Maryland*** 20742

(February 21, 1997)

Abstract

The dependence of the spin polarization on the incident angle of the primary beam has been measured for ^{12}B fragments produced in the fragmentation of an ^{18}O beam on a Nb target at 80 MeV/nucleon. A change in sign of the spin polarization was observed with a change in sign of the incident angle of the projectile. This result is in agreement with the kinematical model presented recently to qualitatively describe the mechanism for the production of spin polarized fragments following intermediate-energy heavy-ion reactions. The resonance curve for ^{12}B has also been measured using a new technique of multiple adiabatic fast passage with continuous implantation. This new technique is briefly compared to the single-pass adiabatic fast passage method

employed with beam-on/beam-off data acquisition.

Typeset using REVTEX

I. INTRODUCTION

Large spin polarization of secondary fragments produced off the central beam axis following intermediate-energy, heavy-ion reactions was first observed by Asahi *et al.* [1]. For ^{12}B fragments produced in the reaction of a 40.6 MeV/nucleon ^{14}N beam on an Au target at an incident beam angle of 5°, sizable polarization (up to 20%) was detected over the whole range of the ^{12}B momentum distribution except at the peak of the momentum yield curve where the polarization was measured to be zero. Dependence of the spin polarization on the residual momentum of the observed fragment was explained using a general kinematical model of projectile fragmentation [1], assuming straight-line trajectories and same-side scattering of the residual fragment away from the target. Considering that the nucleons removed in the fragmentation process are from a localized position within the projectile, coupling the radius vector $\boldsymbol{R}$ describing this position in the projectile rest frame with the momentum vector of the removed nucleons, $\boldsymbol{k}_r$, will constitute the angular momentum of the residual fragment. This resultant angular momentum is dependent on the residual fragment momentum $\boldsymbol{p}_f$ through the relation $\boldsymbol{p}_f = m\boldsymbol{v}_0 - \boldsymbol{k}_r$, where m and $\boldsymbol{v}_0$ are the residual fragment mass and the projectile velocity, respectively. Residual fragments having momenta greater than $m\boldsymbol{v}_0$ will have a preferred orientation of the angular momentum which is of opposite sign to fragments having momenta less than $m\boldsymbol{v}_0$. In addition, residual fragments with momenta equal to $m\boldsymbol{v}_0$ are expected to show no polarization.

The systematic behavior of the spin polarization following projectile fragmentation reactions was measured for different targets and incident beam energies [2]. There was a clear dependence of the spin polarization on both the atomic number of the target and the primary beam energy. In general, it was found that the simple kinematical picture of Asahi *et al.* [1] could predict the gross behavior of the spin polarization of fragments produced in intermediate-energy reactions for light-A projectiles. Some of the observed polarization curves, however, revealed non-zero values for the fragment spin polarization at the peak in the momentum yield curve (where $\boldsymbol{p} = m\boldsymbol{v}_0$). This has been attributed to nucleon rescattering in the residual fragment [2]. This result is significant as secondary fragments could then be produced with large spin polarization at the peak in the production curve, giving assistance to the study of ground state moments of exotic nuclei (see, for example, Ref. [3]).

An additional prediction of the simple kinematical picture of spin polarization produced in projectile fragmentation reactions is that a change in the incident beam angle on target from positive to negative should result in a change in sign of the residual fragment polarization. This point could not be verified in the earlier measurements at RIKEN due to technical limitations on the beam steering dipole magnets located upstream of the RIPS spectrometer target position [4]. In this paper we report measurements of the spin polarization as a function of both the incident beam angle (both positive and negative) on target and the secondary fragment momenta for ^{12}B fragments produced in the reaction of an ^{18}O primary beam at 80 MeV/nucleon on a Nb target.

II. EXPERIMENTAL TECHNIQUE

The experiments were performed using the A1200 fragment separator [5] at the National Superconducting Cyclotron Laboratory (NSCL) at Michigan State University. Secondary ^{12}B fragments were produced using an 80 MeV/nucleon ^{18}O beam provided by the K1200 Cyclotron incident on a 214 mg/cm^2 ^{93}Nb target. Since the A1200 is a zero-degree spectrometer, two dipole magnets located between the exit of the K1200 Cyclotron and the A1200 target box were used to steer the primary beam onto the production target, allowing for the collection of fragments in the range $-3°$ to $+3°$. The horizontal acceptance of the A1200 for the target position in the present experiment was $\approx 1°$, while the momentum acceptance was set to 1% of the central $B\rho$ with a slit at the first momentum-dispersed image of the spectrometer. A 425 mg/cm^2 Al degrader wedge with a slope angle of 3.5 mrad was placed at the second dispersive image of the A1200 to separate fragment isotopes with a given mass-to-charge ratio based on A and Z. Identification of ^{12}B secondary fragments was accomplished at both the A1200 focal plane and the experimental endstation using the energy loss of the fragments measured in 300 μm Si PIN detectors and the fragment time-of-flight (TOF) relative to the K1200 Cyclotron radiofrequency.

The polarization measurements were made using the technique of nuclear magnetic resonance of β-emitting nuclei (β-NMR). A β-NMR endstation has been developed at the NSCL and is similar in many respects to that described by Asahi *et al.* [6]. The β-NMR system is located between the pole faces of a large dipole magnet (pole gap 10.2 cm), which provides the directional holding field and the nuclear Zeeman splitting for the spin-polarized secondary beams. In addition to the dipole magnet, the β-NMR system was comprised of two β detector telescopes, an implantation foil, and a set of radiofrequency (RF) coils. A schematic drawing of the β-NMR system is shown in Fig. 1. The β telescopes each consisted of a 4.4 cm x 4.4 cm x 0.3 cm thick ΔE plastic scintillator and a 5.1 cm x 5.1 cm x 2.5 cm thick total E plastic scintillator. Each scintillator was coupled to a long acrylic light guide (~ 0.5 m) to place the photomultiplier tube of each telescope element beyond the fringe field of the dipole magnet. The β telescopes were placed 9 mm from the center of the implantation foil at 0° and 180° with respect to the direction of the magnetic holding field. The implantation foil was a 2.5 cm x 2.5 cm x 250 μm thick Pt foil which was annealed at 630° C for 10 hours in air. The foil was mounted between the two telescopes and tilted at an angle of 45° relative to the direction of the holding field to reduce the amount of material the β particles had to traverse before reaching the plastic scintillators. The RF coils were two 30-turn loops of 28 AWG magnet wire, arranged in a Helmholtz-like geometry, with a loop radius of 1.2 cm and a separation of 3.0 cm. The coil inductance was measured to be 77 μH, and the coils were placed such that the resulting RF field was perpendicular to the applied field of the dipole magnet.

The RF signal was provided by a Hewlett Packard HP 33120A Function Generator/Arbitrary Waveform Generator and was amplified using an EIN Model 406L RF Power Amplifier. The RF coils were configured as part of an RCL circuit, which included a 50 Ω resistor and a variable capacitor, to provide the maximum possible alternating magnetic field to the sample by matching the impedance of the RF circuit to the output impedance of the

RF source (50 Ω). The strength of the RF field was monitored continuously by measuring the voltage drop across the 50 Ω resistor of the RCL circuit using a Pomona Model 6106 Micro-LC RF detector probe. For the frequencies considered in these measurements, the RF field strength was maintained at ≈ 0.5 mT.

Data acquisition for the ^{12}B polarization measurements required pulsing of the K1200 Cyclotron beam [7]. The time sequence of the beam pulsing is shown in Fig. 2(a). Pulse timing was controlled by the data acquisition computer. For the ^{12}B ($T_{1/2} = 20$ ms) resonance measurements, the implantation (beam-on) time was chosen to be 20 ms and the data collection (beam-off) time was 40 ms. During beam-on cycles, the 35 MeV/nucleon ^{12}B fragments were energy degraded to ≈ 13 MeV/nucleon using Al foils, collimated, and implanted into the Pt catcher foil. Beta particles which produced signals above threshold in both elements of either β telescope were recorded in the event stream during the beam-off cycles only. On alternating beam-off cycles, a frequency-modulated (FM) RF signal was introduced to the implanted sample for the duration of the beam-off period. The ratio of the counting rates in the 0° (Up) and 180° (Down) β telescopes for both RF-on and RF-off conditions

$$R = \frac{(Up/Down)_{\mathrm{RF-on}}}{(Up/Down)_{\mathrm{RF-off}}} \tag{1}$$

is the observed NMR effect, and is related to the magnitude of the fragment polarization.

We have chosen to use a "multiple" adiabatic fast passage (AFP) technique for NMR as opposed to the single-pass AFP technique [8] in the experiments reported here as we were interested in testing an alternative data acquisition method for future β-NMR measurements. In the multiple AFP technique, the FM signal will cause multiple spin-flips of the polarized nuclear state if the resonance falls within the FM band and if the modulation rate is significantly faster than the decay half-life and spin-lattice relaxation time. The net effect of the multiple AFP for a particular nucleus will depend on where the resonance frequency for that nucleus occurs with respect to the FM frequency range. This is shown schematically in Fig. 3. Should the resonance occur at the center of the frequency sweep (position A), then the successive spin flips cause the average spin polarization of the nucleus to be reduced to zero with complete destruction of the β asymmetry. When the nuclear resonance is at frequency B, towards an extremum of the frequency range, two situations can occur as the intervals between successive occurences of such a frequency are unequal (see Fig. 3). If the initial polarized spin (defined here as spin UP) is produced during the longer time interval, two spin flips will occur in rapid succession, resulting in only a small reduction in the average β asymmetry. If, however, the initial production occurs in the shorter time interval, the spin will spend most time DOWN, with consequent average inversion of the asymmetry. A weighted sum of the two possibilities for frequency B will result in a net decrease in the asymmetry, i.e. a net resonance signal. Thus all nuclei having resonant frequencies within the FM sweep range contribute to the total observed resonance signal.

By applying the multiple AFP technique, it was then possible to collect a continuous sample of ^{12}B fragments for a given run with a frequency-modulated RF signal constantly applied to the implanted sample. Normalization of the NMR data was then accomplished by continuously collecting ^{12}B fragments in a second run, this time with no RF signal applied to the sample. The timing sequence used for the continuous implantation with multiple AFP is shown in Fig. 2(b), and was employed to test the feasibility of performing, more efficiently, spin polarization measurements for fragments having half-lives on the order of tens of seconds and longer.

III. RESULTS AND DISCUSSION

A representative resonance curve measured for polarized ^{12}B fragments using the multiple AFP technique and beam-on/beam-off data acquisition is shown in Fig. 4. The goal of this measurement was to verify that we could indeed measure a resonance for a radioactive species with a known magnetic moment. For this resonance, the applied magnetic field was 0.124 T and the incident beam angle on target was +2.5°. The RF signal was frequency modulated using a triangle waveform with a deviation of ± 2 kHz from the central frequency at a rate of 500 Hz. The best fit to the data using a Lorentzian peak shape required a peak centroid of 947.5 kHz and a width of 2 kHz. Using the relation $h\nu_L = gB$, where ν_L is the Larmour frequency corresponding to the peak centroid of the resonance curve, and knowing the ground state spin of ^{12}B is $J^\pi = 1^+$, we deduce a value of $1.003(1)\mu_N$ for the magnetic moment of ^{12}B. This result agrees well with the adopted value [9] of $+1.00306(^{+15}_{-14})\mu_N$ for the magnetic moment of the ground state of ^{12}B.

We measured the spin polarization of the ^{12}B fragments as a function of the longitudinal fragment momenta. Our results are shown in Fig. 5 where the NMR effect is plotted versus the deviation of the ^{12}B fragment momenta from the peak of the momentum yield curve. For the ^{12}B fragments collected at +3° relative to the primary beam axis, one observes that there is polarization of the ^{12}B fragments at the value $\Delta p/p$ = 0%. This confirms the result of Okuno *et al.* [2] that intermediate mass targets produce non-zero values for the polarization at the peak in the momentum yield curve. The polarization of the ^{12}B fragments collected at a beam angle of +3° shows little dependence on the fragment momentum in the range -2% $\leq \Delta p/p \leq$ +2%. This also corroborates the results reported in Ref. [2], where only a small dependence of the ^{13}B polarization was observed over the same range of fragment momenta for the reaction of ^{15}N on ^{93}Nb at 67.3 MeV/nucleon.

The dependence of the ^{12}B polarization on the incident beam angle is also shown in Fig. 5. We observed a change in the sign of the polarization of ^{12}B fragments with a change in the direction of the incident angle of the primary ^{18}O beam from +3° to -2.5°. This result supports the hypothesis in Ref. [1] that the mean deflection angle for the projectile-like fragments, and hence the dominance of near- or far-side trajectories, determines the sign of the observed spin polarization. For ^{12}B fragments collected at 0° relative to the normal beam axis, no polarization was observed. These new results are in agreement with the preliminary results obtained for the production of spin-polarized ^{37}K fragments following high-energy (500 MeV/nucleon) fragmentation [10] at GSI.

An additional result from these measurements was the determination of the resonance curve for ^{12}B using the multiple AFP and continuous implantation. One drawback of single-pass AFP with beam-on/beam-off acquisition is the low duty cycle for data collection. The resonance curve obtained for ^{12}B fragments using multiple AFP and continuous implantation is shown in Fig. 6. Again, the goal of this measurement was not to obtain the best precision nor the best resonance, but to confirm that a resonance measurement is possible using this new technique. The only difference in the experimental conditions for this resonance curve and the resonance curve determined for ^{12}B using multiple AFP and beam cycling (Fig. 4) was the modulation width of the RF signal, which for continuous implanation was $\pm$ 10 kHz. This larger frequency modulation will lead to a broader resonance peak than that observed in Fig. 4, as the asymmetry will be averaged over a wider frequency range. This is reflected in the fit to this data which, when using a Lorentzian peak shape, resulted in a peak centroid of 947 kHz and a linewidth of 7 kHz. The magnitude of the NMR effect for the continuously implanted ^{12}B sample is not significantly different from that measured using the more conventional beam-on/beam-off data acquisition mode. This result suggests that the polarization of the ^{12}B fragments is not affected by the application of an RF field during fragment implantation.

The multiple AFP technique with continuous implantation is expected to provide more efficient data collection for long-lived species. However, it may be inferior to techniques involving beam pulsing in dealing with time-dependent errors. The multiple AFP technique may not be as sensitive to small fragment polarization as single-pass AFP with beam-on/beam-off acquisition. It can be shown [11] that for multiple AFP with continuous implantation, the average spin-flip is only 1/3 of that expected from single-pass AFP. When considering the critical role spin-lattice relaxation plays in determining the feasibility of any polarization measurement [8], techniques involving continuous implantation should be favored. Whereas data are only collected after a fixed beam-on period to allow for sample implanation during beam pulsing, all times following implantation are included when employing the multiple AFP and continuous implantation.

ACKNOWLEDGEMENTS

This work has been supported in part by the National Science Foundation under Contract No. PHY95–28844 (NSCL) and the US Department of Energy under Contract No. DE-FG02-94-ER40834 (U. Maryland). We would like to thank J. Brandon, K. Johnson, and J. Yurkon for their technical assistance, and K. Matsuta for discussions relating the recent β-NMR measurements at Osaka University. We also acknowledge the support of the NSCL operations staff in the successful completion of these measurements.

REFERENCES

[1] K. Asahi, M. Ishihara, N. Inabe, T. Ichihara, T. Kubo, M. Adachi, H. Takanashi, M. Kouguchi, M. Fukuda, D. Mikolas, D. J. Morrissey, D. Beaumel, T. Shimoda, H. Miyatake, and N. Takahashi, Phys. Lett. **B251**, 488 (1990).

[2] H. Okuno, K. Asahi, H. Sato, H. Ueno, J. Kura, M. Adachi, T. Nakamura, T. Kubo, N. Inabe, A. Yoshida, T. Ichihara, Y. Kobayashi, Y. Ohkubo, M. Iwamoto, F. Ambe, T. Shimoda, H. Miyatake, N. Takahashi, J. Nakamura, D. Beaumel, D. J. Morrissey, W.-D. Schmidt-Ott, and M. Ishihara, Phys. Lett. **B335**, 29 (1994).

[3] H. Ueno, K. Asahi, H. Izumi, K. Nagata, H. Ogawa, A. Yoshimi, H. Sato, M. Adachi, Y. Hori, K. Mochinaga, H. Okuno, N. Aoi, M. Ishihara, A. Yoshida, G. Liu, T. Kubo, N. Fukunishi, T. Shimoda, H. Miyatake, M. Sasaki, T. Shirakura, T. Nakahashi, S. Mitsuka, and W.-D. Schmidt-Ott, Phys. Rev. C **53**, 2142 (1996).

[4] T. Kubo, M. Ishihara, N. Inabe, H. Kumagai, I. Tanihata, K. Yoshida, T. Nakamura, H. Okuno, S. Shimoura, and K. Asahi, Nucl. Instr. Methods **B70**, 309 (1992).

[5] B. M. Sherrill, D. J. Morrissey, J. A. Nolen, Jr. and J. A. Winger, Nucl. Instr. Meth. **B56/57**, 1106 (1991).

[6] K. Asahi, M. Ishihara, H. Kamitsubo, N. Takahashi, Y. Nojiri, T. Minamisono, A. Mizobuchi, and K. Sugimoto, Nucl. Instr. Meth. **220**, 389 (1984).

[7] D. Mikolas, B. A. Brown, W. Benenson, L. H. Harwood, E. Kashy, J. A. Nolan, Jr. , B. Sherrill, J. Stevenson, J. S. Winfield, Z. Q. Xie, and R. Sherr, Phys. Rev. C **37**, 766 (1988).

[8] A. Abragam, *The Principle of Nuclear Magnetism* (Clarendon, Oxford, 1961).

[9] P. Raghavan, At. Data Nucl. Data Tables **42**, 189 (1989).

[10] W.-D. Schmidt-Ott, M. Schäfer, T. Dörfler, T. Pfeiffer, K. Asahi, H. Izumi, H. Sato, H.

Ueno, H. Geissel, R. Collatz, M. Hellström, Z. Hum N. Iwasa, M. Pfützner, E. Roeckl, and M. Shibata, *Nachrichten*, GSI Report 12-95, pp. 8-9, 1995.

[11] N.J. Stone, P.F. Mantica *et al.*, to be submitted.

FIGURES

FIG. 1. Schematic of the β-NMR setup at the NSCL.

FIG. 2. Time sequences for ^{12}B β-NMR measurements employing multiple AFP and a) beam cycling, b) continuous implantation.

FIG. 3. Schematic of the effect of mulitple AFP on the spin of a polarized system. The frequency modulation is in the form of a triangle wave, and of interest is the effective spin of the system at positions corresponding to the center of the frequency sweep (position A) and near the extremes of the frequency sweep (position B). The filled arrows indicate the direction of the spin of the polarized ensemble. Details of the multiple AFP method are discussed in the text.

FIG. 4. Resonance curve for ^{12}B using multiple AFP and beam cycling. The frequency modulation was $\pm$ 2 kHz. The dot-dashed line is a Lorentzian fit to the data, which resulted in a peak centroid of 947.5 kHz and a linewidth of 2 kHz.

FIG. 5. Dependence of the spin polarization on the momenta of ^{12}B fragments. Measurements were made for positive deflection (□), negative deflection(×), and normal incidence (○) of the primary ^{18}O beam on the Nb target at 80 MeV/nucleon. The applied RF for all data points was set to the resonance peak for ^{12}B, with a frequency modulation of $\pm$ 30 kHz. The values $\Delta p/p$ give the deviation of the momentum of ^{12}B fragments from the peak of the momentum yield curve. The error bars on these values indicate the momentum acceptance of the A1200.

FIG. 6. Resonance curve for ^{12}B using multiple AFP and continuous implantation. The frequency modulation employed was $\pm$ 10 kHz. The dot-dashed line is a Lorentzian fit to the data, which resulted in a peak centroid of 947 kHz and a linewidth of 7 kHz.

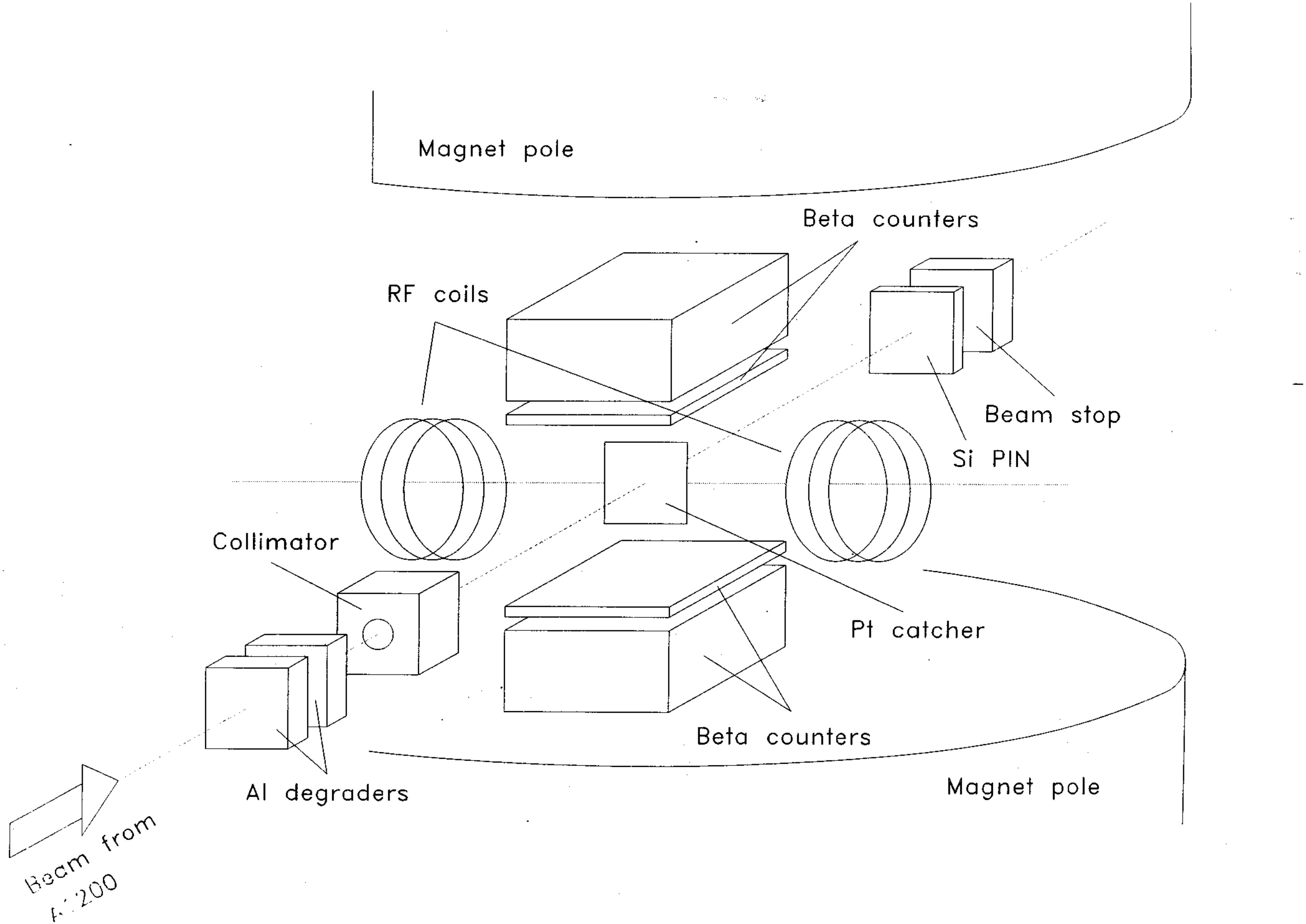
Magnet pole
Beta counters
RF coils
Beam stop
Si PIN
Collimator
Pt catcher
Beta counters
Al degraders
Magnet pole
Beam from

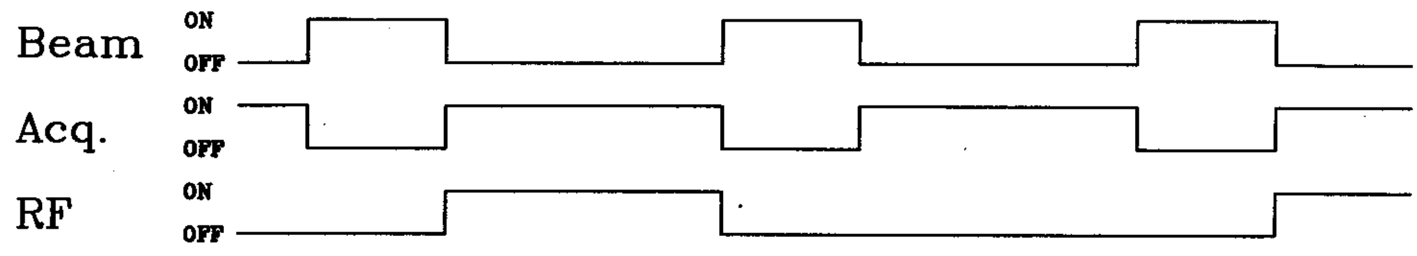

(a) Beam Cycling

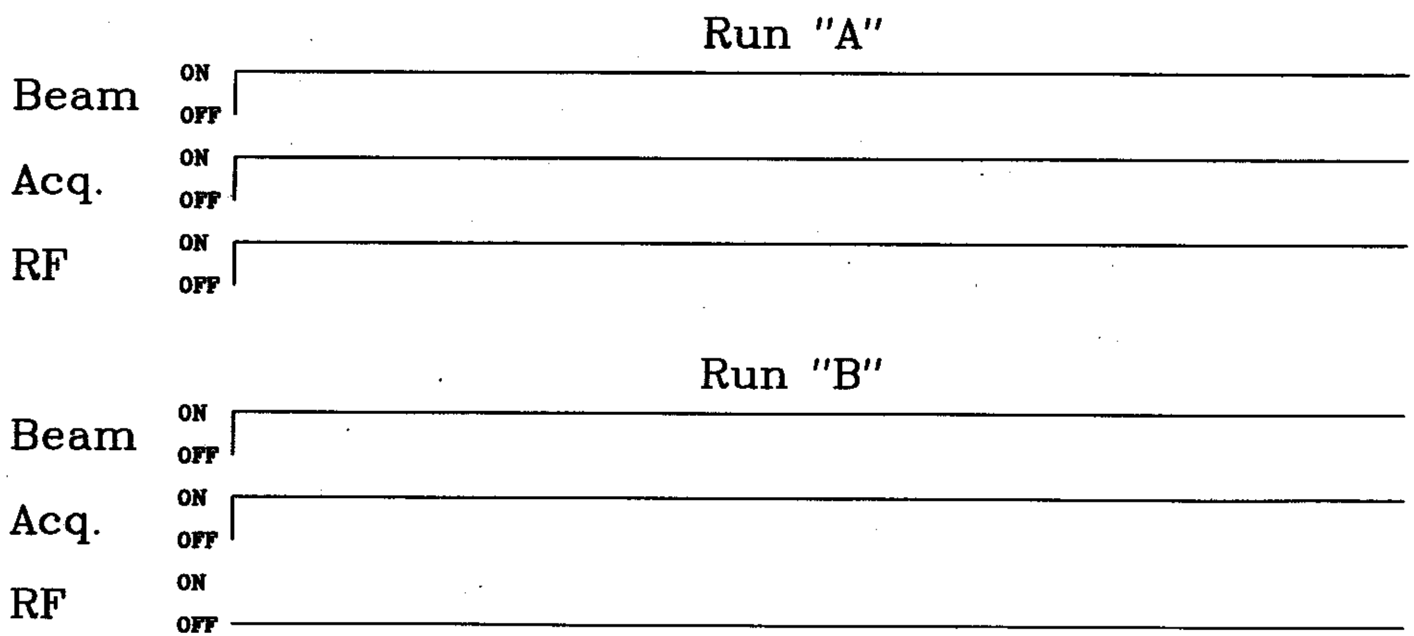

(b) Continuous Implantation

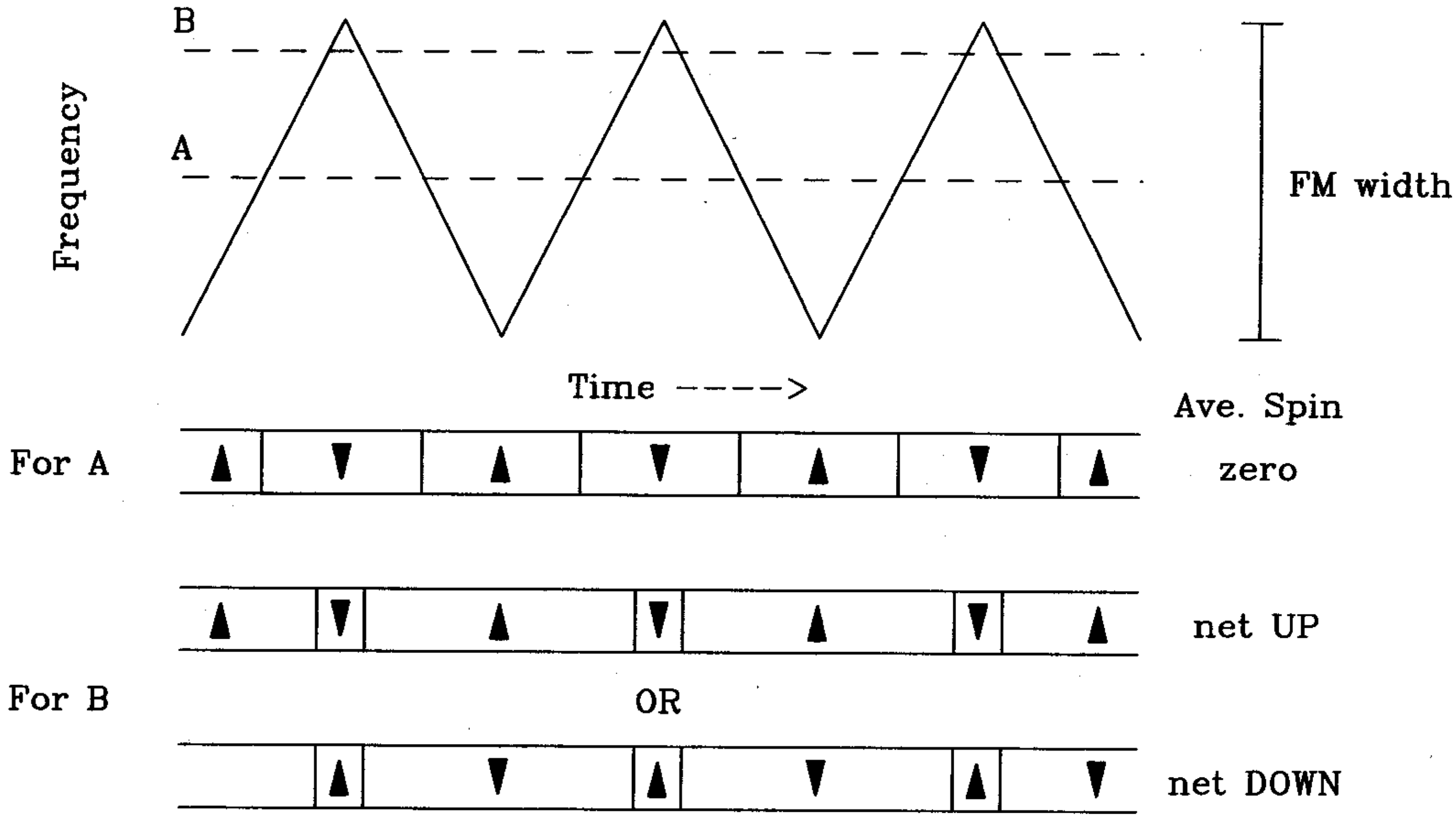
B
A
Frequency
FM width
Time ---->
Ave. Spin
For A
zero
net UP
For B
OR
net DOWN

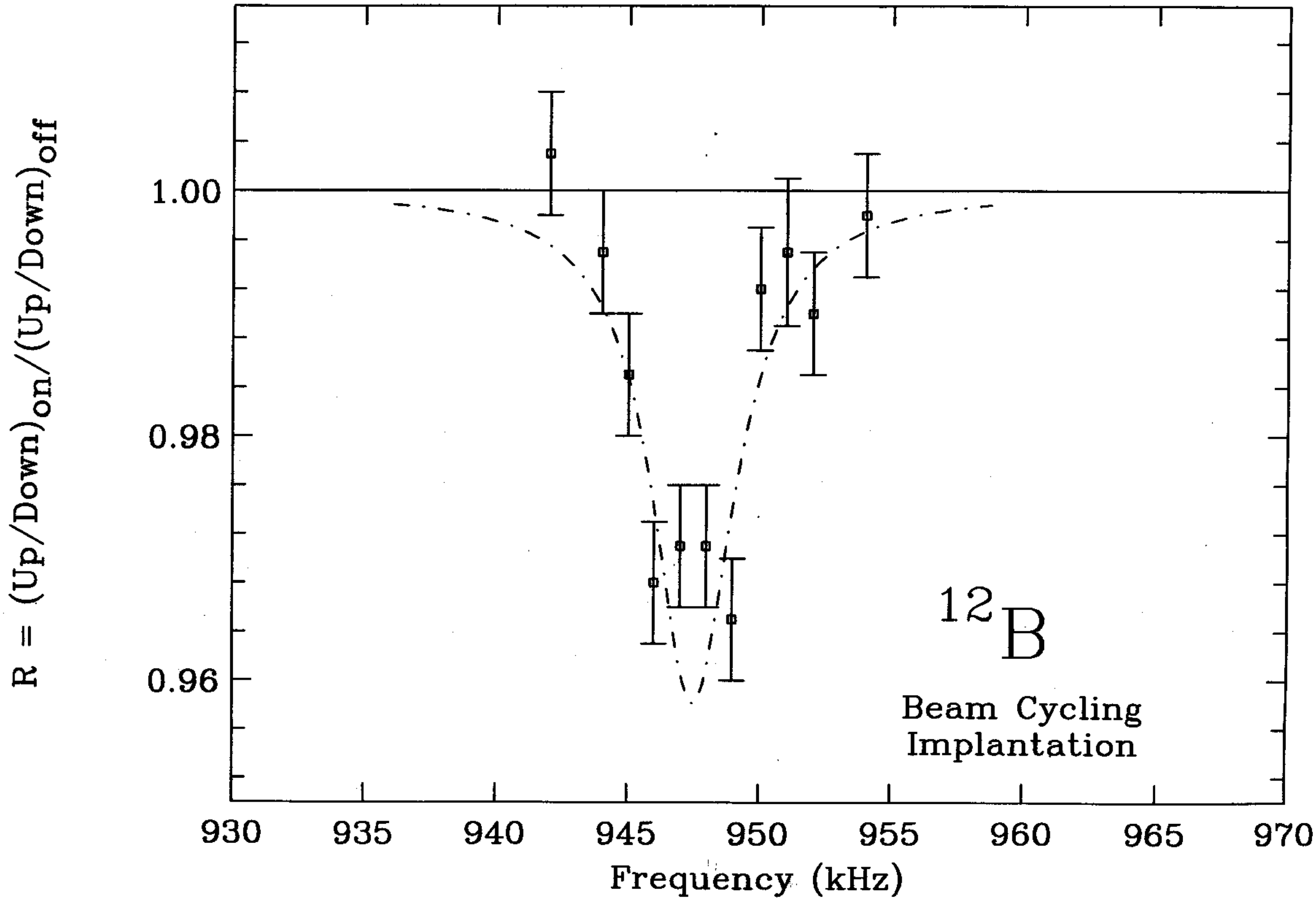

R = (Up/Down)on/(Up/Down)off
1.00
0.98
0.96
930
935
940
945
950
955
960
965
970
Frequency (kHz)
12B
Beam Cycling
Implantation

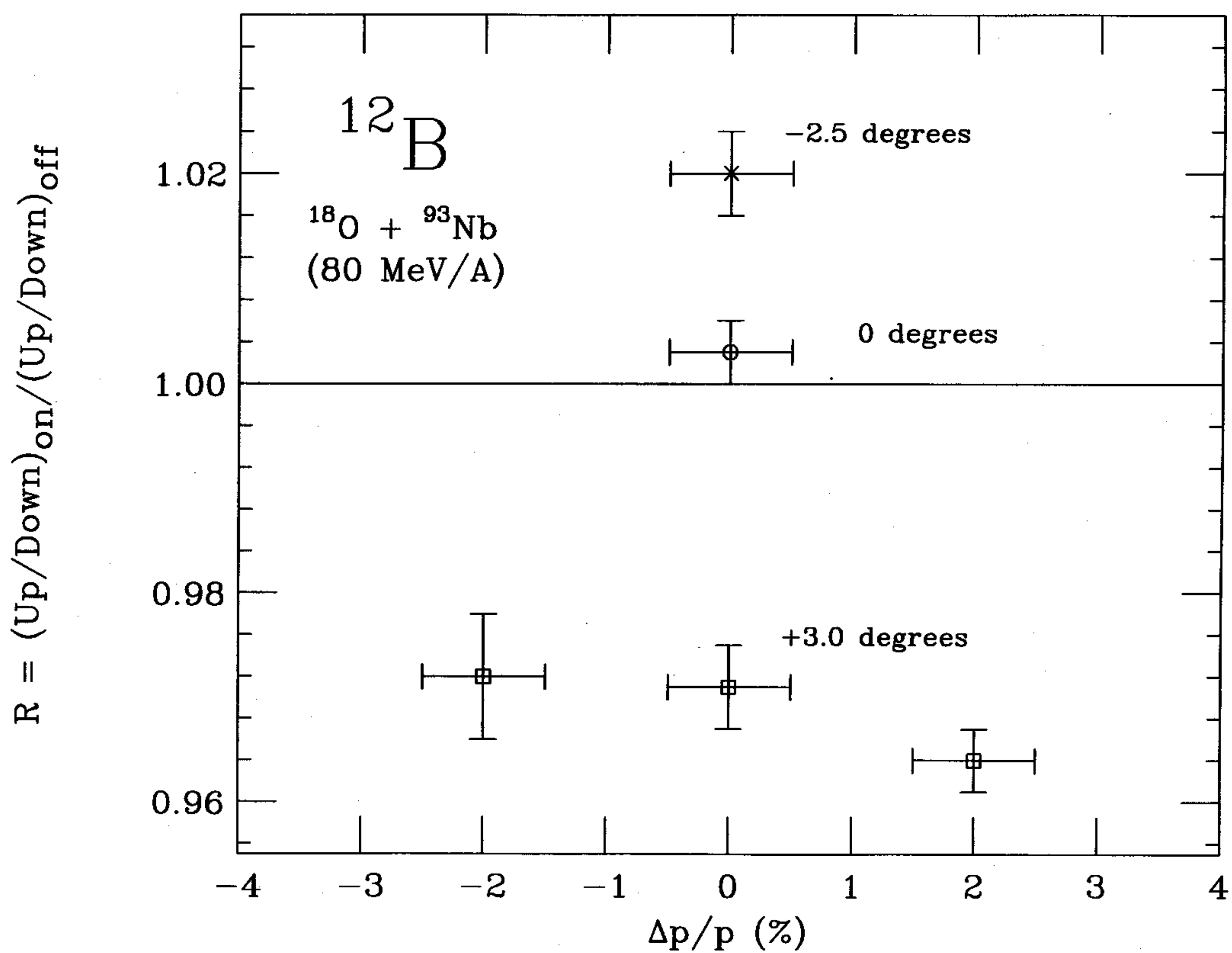

^{12}B
^{18}O + ^{93}Nb
(80 MeV/A)
−2.5 degrees
0 degrees
+3.0 degrees
1.02
1.00
0.98
0.96
−4
−3
−2
−1
0
1
2
3
4
Δp/p (%)
R = (Up/Down)$_{on}$/(Up/Down)$_{off}$

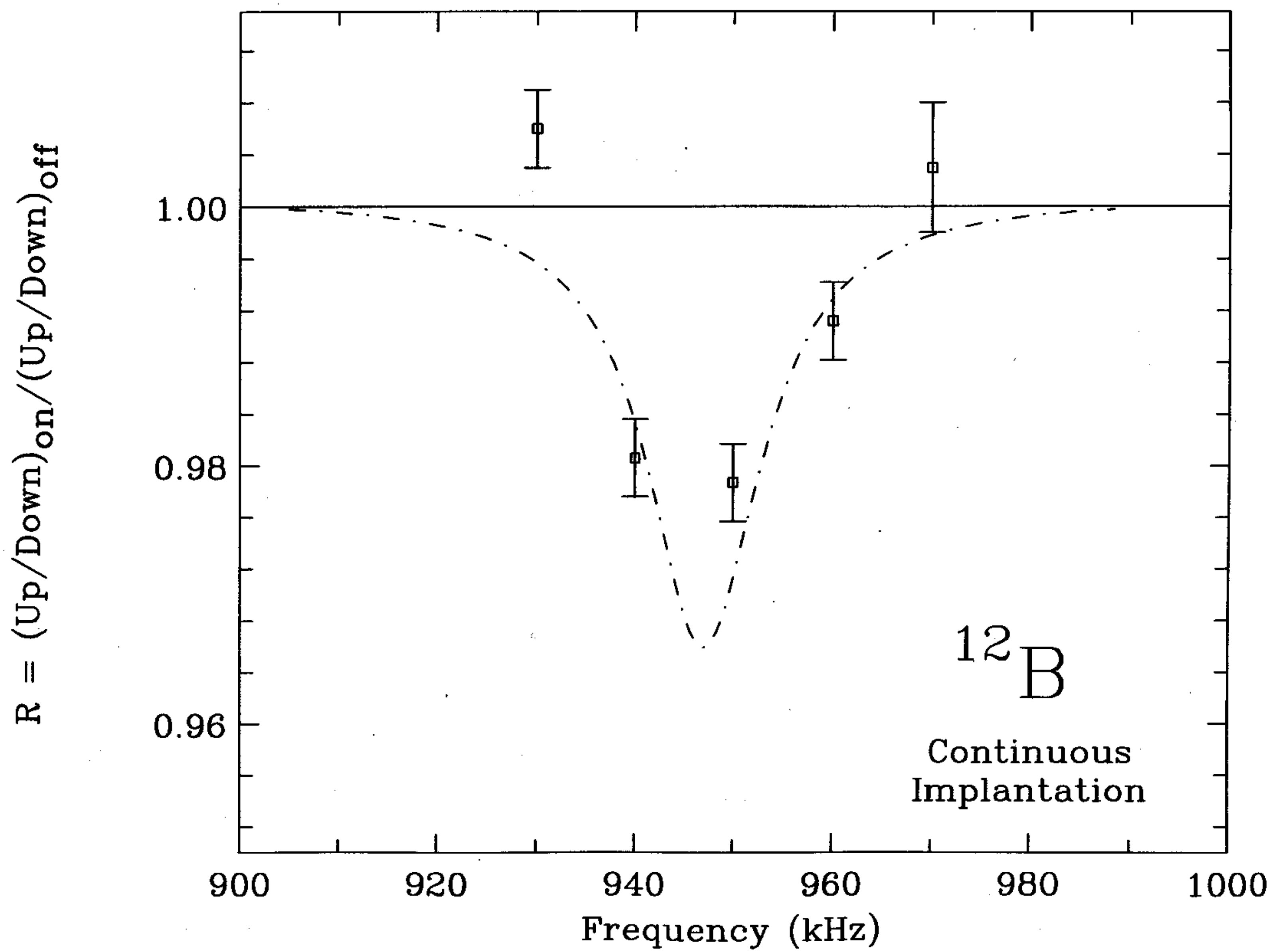
R = (Up/Down)on/(Up/Down)off
1.00
0.98
0.96
900
920
940
960
980
1000
Frequency (kHz)
12B
Continuous
Implantation